

## Synthesis and Evaluation of Nano Zeolite Na/Al as a New Modifier for Electrochemical Determination of Acetaminophen

Afroozeh Arabi<sup>1</sup>, Alireza Mohadesi<sup>\*1</sup>, Mohammad Ali Karimi<sup>1</sup>, Mehdi Ranjbar<sup>2</sup>

1. Department of Chemistry, Payame Noor University, Tehran 19395-4697, Iran

2. Pharmaceutics Research Center, Institute of Neuropharmacology, Kerman University of Medical Sciences, Kerman, Iran

Received: 10 January 2022

Accepted: 27 February 2022

DOI: 10.30473/ijac.2022.64005.1238

### Abstract

In this study, a new Zeolite Al/Na (ZAN) was synthesized and characterized and then a new modified Carbon Paste Electrode with ZAN was made to determine Acetaminophen. Electrochemical studies using Linear Sweep Voltammetry and differential pulse voltammetry were used to determine electrochemical Acetaminophen. In the presence of Acetaminophen, modified electrode with ZAN shows a specific anodic peak at ~ 0.59 volts which is the result of using electrocatalytic oxidation of Acetaminophen. The determination limit of this method to measure Acetaminophen was 5.8  $\mu$ M, the relative standard deviation for 7 repeated measurements was 1.1 % and linear range of the calibration to measure Acetaminophen was 10 up to 115  $\mu$ M.

### Keywords

Zeolite Al/Na; Carbon Paste Electrode; Acetaminophen; Electroanalysis.

### 1. INTRODUCTION

Fig. 1. shows acetaminophen (AC) or paracetamol and is used all over the world as a non-carcinogenic drug with antipyretic and analgesic properties and it is also the best alternative to aspirin [1-3].

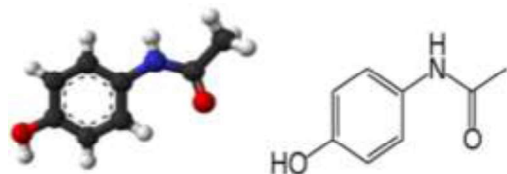


Fig. 1. Structure of AC

The mechanism of AC action is not well understood, but its effect seems to be due to the reduced production of prostaglandins in the body which are the main causes of inflammation and fever [4-6]. AC reduces the production of this substance in the central nervous system [7], the brain and spinal cord [8-10]. Excessive use of AC causes toxins to accumulate in the liver and kidneys because the liver is the center of AC change metabolism [11, 12]. Therefore, it is necessary to use fast, accurate and simple methods for measuring AC [13]. The types of methods used to measure AC are: titrimetry [14, 15], Fourier transform infrared spectroscopy [16, 17], mass spectrometry [18, 19], fluorometry [20, 21], electrochemical [22-24], chromatography [25-27],

visible-ultraviolet spectrophotometry and many others, but the electrochemical method in [27, 28] which the modified electrode was used is more common because it is reproducible, sensitive, and simple.

A large increase in surface sensitivity and a significant reduction in interference effects and determination limit can be achieved by modifying the electrode surface. Zeolites were invented in 1756 by Axel Frederick Kronstadt [29]. They are consist of channels or holes with a diameter from 0.3-1.5 nm and have three-dimensional networks consist of  $[\text{SiO}_4]^{4-}$  and  $[\text{AlO}_4]^{4-}$  (30, 31). They are generally divided into natural and artificial. natural Zeolites are formed in open groundwater systems, alkaline lakes, deep-sea sediments and alkaline soils [29]. Due to the importance of synthetic Zeolites, their number was increasing day by day, because many disadvantages of natural Zeolites such as: uneven pore size, abundant impurities, insufficient pore size and unsuitable surface acidity were eliminated and up to 4 The categories were divided [32]. These are: Zeolite with small pores [33], Zeolite with medium pores [34, 35], Zeolite with large pores [36, 37] and Zeolite with very large pore size [38]. Its main application is as a surface adsorbent and catalyst and it is used in various cases such as: production of laundry detergents [39], water purification [40], medicine and agriculture [41]. It can also trap heavy toxic elements [42]. Another usage of Zeolite is: using

\*Corresponding Author: mohadesi@pnu.ac.ir

to harden water. In chemistry, it is used to separate molecules as a trap for the release of molecules and their analysis [43]. It has the ability to accurately separate gases from natural gas and can compete with fluorescent or LED lights with the help of natural silver emitting light [44]. In oxygen generators [45], zeolite is used along with the nitrogen uptake system from the air to supply oxygen to the aircraft [46].

For more than five years, carbon paste electrodes (CPEs), a combination of carbon powder and binder, have been considered by many chemists as electrode former material for sensors and detectors [47]. This attention is definitely due to the physical, chemical and electrochemical properties of this compound. These electrodes are generally very compatible with chemical modification. Modifiers such as nanomaterials, zeolites, metal complexes and organic compounds have been used to modify the properties of carbon paste [48]. In general, chemically modified electrodes have less determination limit than unmodified electrodes. Zeolite modified electrodes are a subset of chemically modified electrodes [49, 50] and they are made in different ways in chemistry which are: covalent bonding of Zeolite particles with the electrode surface [51], stabilization of Zeolite on the conductive surface [52], dispersion of Zeolite particles in graphite and coating on solid electrode with Zeolite [53, 54]. They also have advantages and can be distinguish between small reactants by combining the specific molecular sieve properties of zeolite and ion exchange voltammetry [55]. Another reason for the superiority of zeolite modified electrodes is the combination of important properties of zeolites such as size selection, ion exchange capacity, high thermal and chemical stability with new high-sensitivity electrochemical techniques which significantly improve [56, 57] chemically modified electrodes compared to other sensors. The possible use of zeolite modified electrodes in electrocatalysis is another reason to study them. Zeolites can support different catalysts in different locations with a three-dimensional lattice due to their selectivity based on the size and shape of the reactants [58]. Zeolites of supported metal cations are widely used as effective electrocatalysts due to the electrocatalytic properties of intermediate metal cations to modify different electrode levels in the voltammetric and amperometric determination of various medicine compounds and other chemical compounds [59, 60]. In modified electrodes, the intermediate metal cations can act as electrocatalysts for the analyte molecules at the electrode-solution junction, which are removed from the zeolite channels through the ion exchange process with the cations in the backing electrolyte

solution [61].

In this research, an attempt was made to synthesize and characterized nano zeolite Al/Na (ZAN) and then it was used as a modifier in the texture of carbon paste electrode modified with zeolite Al/Na (ZAN-CPE) and finally the resulting electrode was used to measure AC electrochemically.

## 2. EXPERIMENTAL

### 2.1. Apparatus

Samsung microwave, Sigma3-16L centrifuge and Shimadzu vacuum oven were used to synthesize ZAN. Voltammetry experiments were performed using a Metrohm 797 VA electro-analyzer with a three-electrode system consist of a platinum wire as the counter electrode, a CPE as the working electrode and an Ag/AgCl electrode as the reference electrode. All experiments were performed in the presence of pure nitrogen. Metrohm 710 was used to set-out the pH. The X-ray diffraction patterns were used to phase characterize the Al/Na nanostructure zeolites. The scanning electron microscopy (SEM, JXA-8100 and JSM-6700F) were used to characterization of morphology and surface properties. The Fourier-transform infrared spectroscopy (FT-IR) spectra were recorded on Magna-IR, spectrometer 550 Nicolet in KBr pellets in the range of 400-4000  $\text{cm}^{-1}$ .

### 2.2. Materials

The materials used in this research are: Paraffin Oil (99%, Sigma-Aldrich), Graphite powder (99% carbon with mesh size 200, Merck), Potassium Chloride (99%, Sigma-Aldrich), Ammonium Chloride (Merck, 99.5%), Sodium Acetate (Merck, 99%), Phosphoric Acid (Merck, 85%), Sulfuric Acid (Merck, 98%), AC (99.9%, Merck), Sodium Chloride (Merck, 99%), Ethanol (96%, Merck), Aluminum Chloride (Merck, 25%), Sodium Silicate (99%, Merck), Sodium Dodecyl Sulfate (Merck, 85%) and Deionized Water.

### 2.3. Synthesis of ZAN

0.5 gr of Aluminum Chloride in Deionized Water and Ethanol was dissolved in a certain ratio of 1: 2, then 2 M solution of Sodium Hydroxide was added to this solution. The process of co-precipitation and nucleation in aqueous conditions was obtained by set-out NaOH. 0.05 gr of Sodium Silicate was dissolved in 3 ml of water and then refluxed at 50 °C for 45 minutes. When necessary, 1 M NaOH was added to the solution to set-out the pH to 6 to 7 in the reaction medium. During the process, 0.01 gr of SDS was added to the final solution. After nucleation, we investigated Zeolite nanostructures under microwave conditions for a specific time and power. This stage was due to the explosion of the grown nuclei with discoloration. After the thermal

steps were completed, the reaction mixture was cooled to ambient temperature and the white solid particles were precipitated by the addition of Ethanol and separated by centrifugation. After the separation step, the product was washed several times with Ethanol to remove impurities and dried in a vacuum oven at 50 °C.

#### 2.4. Preparation of ZAN-CPE

To prepare CPEs, 1 gr of Graphite powder with 0.01 g of ZAN was poured into a hand mortar and mixed with a grinder. Then 25% by weight of Paraffin Oil was added to the resulting mixture. Insert the prepared carbon paste into the open and perfectly smooth end of a glass tube with a diameter of 2 mm, and by polishing its surface on white paper, a glossy, perfectly smooth and uniform surface was obtained. For the electrical connection of the electrode, copper wire was used, which was placed inside the glass tube on one side and connected to the carbon paste, and on the other side, it was connected to the electrochemical device by an interface. The structure of the electrode seems that it can be acting like a piston. In this way, by pressing the copper wire inside the pipe downwards, the carbon paste at the end of the pipe was easily separated from the pipe and its surface was renewed. Also for comparison work, zeolite-free carbon paste electrodes were made in a similar way to zeolite-modified electrodes.

#### 2.5. Electrochemical determination of AC

For AC differential pulse voltammetric (DPV) tests, 20 ml phosphate buffer 0.1 M with pH 6 was dumped into an electrochemical cell. Potential was scanned from 0.3 to 1.2 V (with scan rate of 25 mV/s). The peak current for the modified electrode in the AC compound appeared at a potential of ~0.59 volts. Then different amounts of AC solution were added to the cell and scanned. All determinations were performed at room temperature. It was kept outdoor in the open air when the modified electrode not used.

### 3. RESULT AND DISCUSSION

#### 3.1. Characterization of ZAN

Fig. 2. shows SEM image related to ZAN nanostructure before thermal step (sample 1) and after thermal step (sample 2) respectively.

Fig. 3. Shows DLS diagram distribution statistics are Dn 10%: 135.68 nm, Dn 50%: 411.58 nm and Dn 90%: 495.2 nm. This indicates that the particles have been synthesized with perfectly uniform dispersion and in the particle size range ~ 200-400 nm.

Fig. 4. Shows FTIR spectroscopy of the as-synthesized ZAN nanostructure samples was evaluated. Absorption peak at 2926  $\text{cm}^{-1}$  and 2853  $\text{cm}^{-1}$  are related to C-H band trapped in the

molecule structure of the surface structures. The typical absorbance at 2175  $\text{cm}^{-1}$  proved the presence of the C-C in nanostructure. A weak peak appeared in 1459  $\text{cm}^{-1}$  is related C=O stretching vibrations and symmetric stretching vibration band. The absorption bands at about 615.25  $\text{cm}^{-1}$  can be related to Na/Al in ZAN nanostructure.

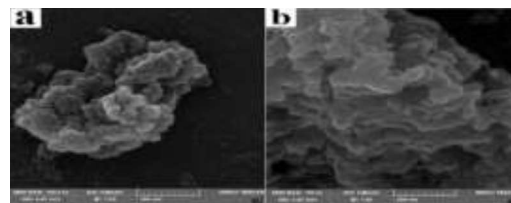


Fig. 2. SEM image of zeolite Na/Al nanostructure relate to before thermal step (a) and after thermal step (b).

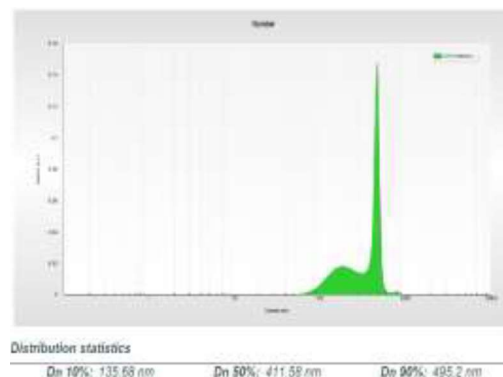


Fig. 3. DLS diagram of the synthesized zeolite Na/Al nanostructure.

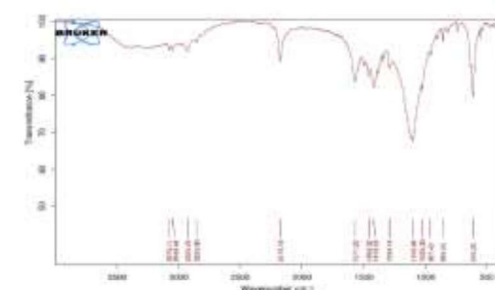
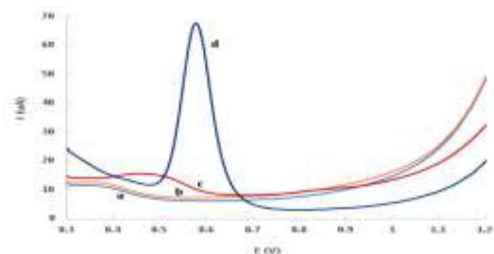


Fig. 4. FT-IR spectroscopy of zeolite Na/Al nanostructure.

#### 3.2. Study of voltammetric behavior:

The first, the response of an unmodified CPE and the response of a ZAN-CPE in the presence and absence of AC were evaluated by DPV. As shown in figure 5, the response obtained in 0.1 M molar phosphate solution on the unmodified CPE surface (curve a) indicates a complete lack of electrochemical activity of the electrode in the potential range of 0.3 to 1.2 volts. Curve b shows that CPE after the addition of AC, like CPE in the absence of AC, does not have electrochemical activity in the specific range. Curve c shows the voltammetric response of ZAN-CPE in the

absence of AC. It shows that an anodic broad peak in ~500 mV is due to the electrochemical activity of Zeolite in this range. Curve d shows the ZAN-CPE voltammetric response in the presence of AC in which the maximum anodic current occurs in ~590 millivolts, and this electrocatalytic effect is related to the oxidation of AC in ZAN-CPE surface. The reason for the increase in anodic current may be due to the high surface to volume ratio and high porosity in ZAN-CPE.



**Fig. 5.** DPVs in 0.1 M phosphate buffer with pH 6 in: (a) CPE in the absence of AC, (b) CPE in the presence of 80  $\mu$ M AC, (c) ZAN-CPE in the absence of AC and (d) ZAN-CPE in the presence of 80  $\mu$ M AC.

Fig. 6. shows the effect of scanning speed on the electrochemical behavior of 25  $\mu$ M AC solution under optimal conditions and in phosphate buffer pH=6. Fig. 6A. shows the linear sweep voltammetries (LSVs) from 10 to 100 mV/s and shows that the anodic peak currents associated with AC oxidation increases with increasing scan speed.

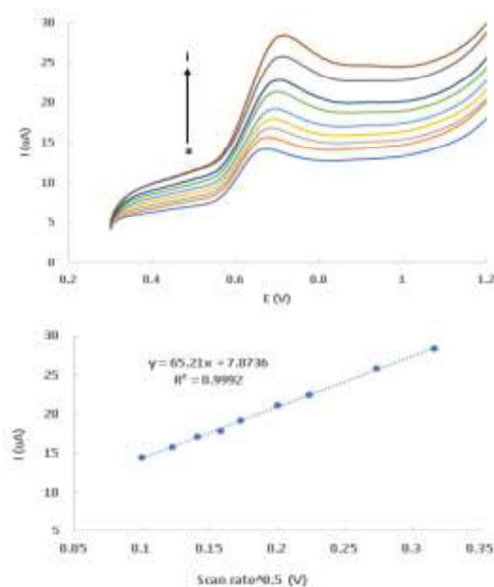


**Fig. 6.** (A) LSVs of ZAN-CPE in 25  $\mu$ M AC in phosphate buffer pH 6 with different scanning speeds a to i: 10, 15, 20, 25, 30, 40, 50, 75 and 100 mV/s, (B) the graph of anodic peak currents versus square root of scan rates.

As shown in Fig. 6B. the linear relationship between the flow changes is in terms of the square of the scan speed and according to the equation  $I = 62.21v + 7.87$  and the regression coefficient 0.999. These results show that the oxidation of AC is controlled by diffusion.

### 3.3. Influences of pH and Zeolite amount

As shown in fig. 7A. the influence of the pH of the solution on the electrochemical oxidation of AC was examined. This study was performed in the range of 2.0 to 13.0 using DPV and it was found that in acidic media the maximum peak oxidation is higher than in alkaline medium. In the pH range between 2 and 5, the anodic peak flow increased gradually and slowly. The highest catalytic current was observed at pH 6 and was selected as the optimal pH. At pH > 6 the anodic peak current decreased. The reason for the decrease in current was that protons participate in electrochemical reactions, and the greater the involvement of protons in the oxidation of acetaminophen, the lower the anode current peak, and eventually the peak was removed.

As the results show in fig. 7B. the next influential factor that was investigated was the effect of the amount of ZAN used in the construction of ZAN-CPE. What is clear is that the anodic peak current associated with AC oxidation changed as a function of the amount of ZAN. When the carbon electrode was modified with 1-2% g ZAN, the anodic peak current increased due to the increased catalytic effect of the modifier and then decreased by 2% due to the arrival of the modifier.

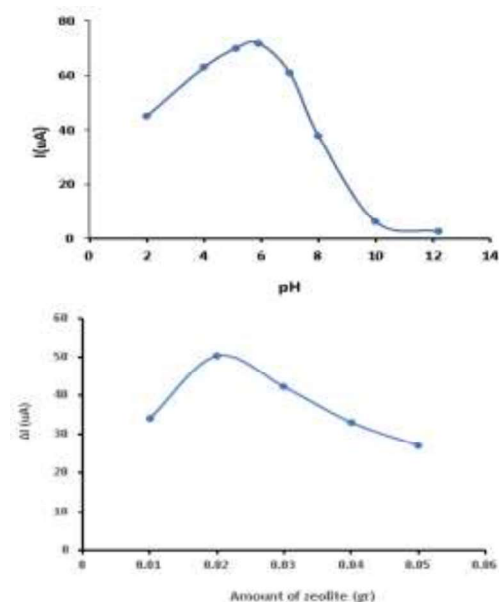


**Fig. 7.** The effect of the pH (A) and the amount of modifier, ZAN (B) on the electrode response.



3.4. Calibration curve, reproducibility, detection limit and interferences

Fig. 8. shows the AC calibration curve. According to fig. 8A. different concentrations of AC in the range of 10-115  $\mu\text{M}$  were prepared and the desired DPVs were recorded. Fig. 8B. shows the linear dependence between the anodic peak currents in terms of different concentrations of AC, and the results were expressed by the line equation  $I = 0.62C + 19.08$  and the regression coefficient 0.999. To evaluate the accuracy of the method, AC solution with a concentration of 80  $\mu\text{M}$  was prepared and after seven measurements under optimal conditions, the relative standard deviation (RSD) of 1.1% was calculated. Seven control solutions were prepared to computation the detection limit. The detection limit of AC was 5.8  $\mu\text{M}$ .

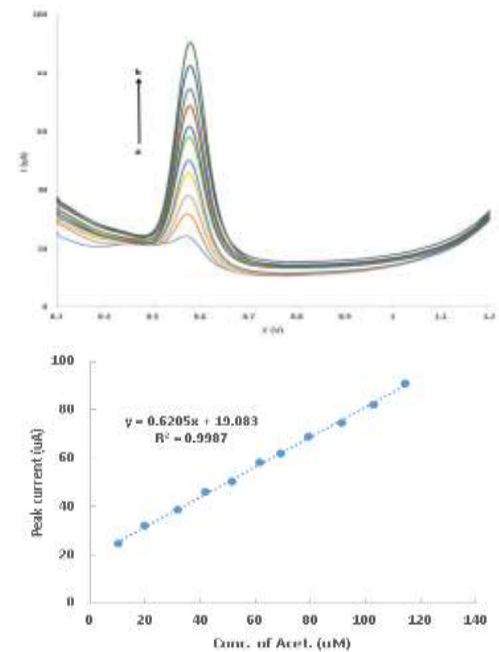


Fig. 8. (A) DPVs with different concentrations of AC, (B) anodic peak currents against concentration of AC.

Table. 1. shows the study of disturbing species. The reason for this study is to investigate the anti-interference ability of the electrode modified with ZAN. The studied species were Morphine, Rutin, Glucose, Folic Acid, Amoxicillin Hydrate, Tyrosine and Tryptophan. 500  $\mu\text{M}$  of these disturbing species were added to the phosphate solution containing 50  $\mu\text{M}$  of AC. The AC in the phosphate solution was then measured by the modified electrode. As the results show, these compounds do not have a significant effect on the measurement of AC and their limit is proportional to each compound, causing a less than  $\pm 5\%$  error in the AC signal.

Table. 1. The effect of disturbances

Species	Recovery
Morphine	100
Rutin	105
Glucose	96
Folic Acid	95
Amoxicillin Hydrate	100
Tyrosine	100
Tryptophan	99

3.5. Real sample analysis

As an applied view, the method presented in this study was used to measure AC in some drug samples including cold stop pills and acetaminophen codeine pills. The powder of each real sample was diluted with phosphate buffer solution ( $\text{pH} = 6$ ). AC concentrations were measured using the standard increment method for each sample. To evaluate the application of the proposed method, AC recoveries were also determined in different drug samples. Recovery results are between 99 to 102%. Table. 2. shows that the proposed ZAN-CPE has good application for measuring AC in real samples.

Table. 2. Determination of AC in real samples (n=3).

Real sample	AC added ( $\mu\text{M}$ )	AC found ( $\mu\text{M}$ )	Recovery (%)	RSD (%)
AC codeine pills	0	19.4	-	1.9
	20	39.2	99.5	2.3
	50	69.1	99.6	2.7
	70	88.6	99.1	2.5
	0	27.6	-	2.1
Cold stop pills	20	48.5	101.9	2.5
	50	77.3	99.6	2.6
	70	98.2	100.6	2.8

4. CONCLUSION

In this study, a new nano zeolite Al/Na was synthesized. Characterization of this zeolite was performed by SEM, FTIR and DLS. In the following an effective and new method for measuring acetaminophen was presented based on carbon paste electrode modified with this zeolite Al/Na. This modified electrode showed good behavior for measuring acetaminophen in small quantities of drug samples. According to the results of Table 3, it is clear that the proposed method has the good detection limit and comparative linear range.

Table. 3. Comparison of the performance of several reported methods for determination of AC

Methods	Detection limit ( $\mu\text{M}$ )	Linear range ( $\mu\text{M}$ )	Ref.
PMG/f-MWCNT/GC	4.3	25-200	[45]
MWCNT/TiO <sub>2</sub> /GCE	11.7	10-120	[46]
CB(BP)/SPE	2.6	4-80	[47]
ZAN-CPE	5.8	10-115	This work

# REFERENCES

- [1] DY. Naumov, M.Vasilchenko and J. Howard. The monoclinic form of acetaminophen at 150K. *Acta. Crystallogr. C*. 5;54 (1998) 653-5.
- [2] SR. Perumalla, L. Shi and C.C. Sun. Ionized form of acetaminophen with improved compaction properties. *CrystEngComm*. 7;14 (2012) 2389-90.
- [3] K. Kawabata, K. Sugihara, S. Sanoh and S. Kitamura. Ultraviolet-photoproduct of acetaminophen: Structure determination and evaluation of ecotoxicological effect. *J. Photoch. Photobio A*. 249 (2012) 29-35.
- [4] RM. Botting. Mechanism of action of acetaminophen: is there a cyclooxygenase 3? *CLIN. INFECT DIS*. 5;31(2000) S202-S10.
- [5] BJ. Anderson. Paracetamol (Acetaminophen): mechanisms of action. *Pediatr. Anesth*. 10;18 (2008) 915-21.
- [6] O.Bandschapp, J. Filitz, A. Urwyler, W. Koppert and W. Ruppen. Tropisetron blocks analgesic action of acetaminophen: a human pain model study. 6;152(2011) 1304-10.
- [7] J.P. Courade,D. Besse. C. Delchambre, N. Hanoun. M, Hamon and A. Eschaliel. Acetaminophen distribution in the rat central nervous system. *Life. Sci*. 12; 69 (2001) 1455-64.
- [8] M.H.da Silva, E.J.F. da Rosa, N.R. de Carvalho, F. Dobrachinski, J.B.T. da Rocha and J.L. Mauriz. Acute brain damage induced by acetaminophen in mice: effect of diphenyl diselenide on oxidative stress and mitochondrial dysfunction. *Neurotox. Res*. 3;21 (2012) 334-44.
- [9] P. Honoré, J. Buritova and J.M. Besson. Aspirin and acetaminophen reduced both Fos expression in rat lumbar spinal cord and inflammatory signs produced by carrageenin inflammation. *Pain*. 3;63 (1995) 365-75.
- [10] C.I. Ghanem, M.J. Pérez, J.E. Manautou and A.D. Mottino. Acetaminophen from liver to brain: New insights into drug pharmacological action and toxicity. *Pharm. Res*. 2016; 109:119-31.
- [11] G. Şener, A.O. Şehirli and G. Ayanoğlu-Dülger. Protective effects of melatonin, vitamin E and N-acetylcysteine against acetaminophen toxicity in mice: a comparative study. *J. Pain. Res*.1;35 (2003) 61-8.
- [12] H.L. Bonkovsky, R.E. Kane, D.P. Jones, R.E. Galinsky and B. Banner. Acute hepatic and renal toxicity from low doses of acetaminophen in the absence of alcohol abuse or malnutrition: evidence for increased susceptibility to drug toxicity due to cardiopulmonary and renal insufficiency. *Hepatology*. 5;19 (1994) 1141-8.
- [13] H. Montaseri and P.B. Forbes. Analytical techniques for the determination of acetaminophen: A review. *T.r.A.C.* 108 (2018) 122-34.
- [14] G. Burgot, F. Auffret and J.L. Burgot. Determination of acetaminophen by thermometric titrimetry. *Anal. Chim. Acta*. 2;343 (1997) 125-8.
- [15] C.B. Choi, J.S. Song, Y.M. Kang, C.H. Suha, J. Lee and J.Y. Choe. A 2-week, multicenter, randomized, double-blind, double-dummy, add-on study of the effects of titration on tolerability of tramadol/acetaminophen combination tablet in Korean adults with knee osteoarthritis pain. *Clin. Ther*. 7;29 (2007) 9-1381.
- [16] A. Rahman. Application of fourier transform infrared spectroscopy for quality control of pharmaceutical products: a review. *Indonesian. J. Pharm*. 1;23 (2012) 1-8.
- [17] R. Gautam, B. Chandrasekar, M. Deobagkar-Lele, S. Rakshit, B.N.V. Kumar and S. Umapathy. Identification of early biomarkers during acetaminophen-induced hepatotoxicity by Fourier transform infrared microspectroscopy. *plos one* . (2012).
- [18] M.C. Damsten, J.N. Commandeur, A. Fidder, A.G. Hulst, D. Touw and D. Noort. Liquid chromatography/tandem mass spectrometry detection of covalent binding of acetaminophen to human serum albumin. *Drug. Metab. Dispos*. 8;35 (2007) 1408-17.
- [19] Y. Zhang, N. Mehrotra, N.R. Budha, M.L. Christensen and B. Meibohm. A tandem mass spectrometry assay for the simultaneous determination of acetaminophen, caffeine, phenytoin, ranitidine, and theophylline in small volume pediatric plasma specimens. *Clin. Chim. ACTA*. 2;398 (2008):105-12.
- [20] M.L. Helaleh and T. Korenaga. Fluorometric determination of nitrite with acetaminophen. *Microchim. J*. 3;64 (2000) 241-6.
- [21] X. Bu, Y. Fu, X. Jiang, H. Jin and R. Gui. Self-assembly of DNA-templated copper nanoclusters and carbon dots for ratiometric fluorometric and visual determination of arginine and acetaminophen with a logic-gate operation. *Microchim. ACTA*. 3;187 (2020) 1-10.
- [22] S. Lotf and H. Veisi. Pd nanoparticles decorated poly-methyldopa@ GO/Fe3O4 nanocomposite modified glassy carbon electrode as a new electrochemical sensor for simultaneous determination of acetaminophen and phenylephrine. *Model. Simul. Mater Sc*. 105 (2019) 110-112.

- [23] R. Chokkareddy, N. Thondavada, N.K. Bhajanthri and G.G. Redhi. An amino functionalized magnetite nanoparticle and ionic liquid based electrochemical sensor for the detection of acetaminophen. *Anal. Methods*. 48;11 (2019) 6204-12.
- [24] Y. Sun, J. He, G.L. Waterhouse, L. Xu, H. Zhang and X. Qiao. A selective molecularly imprinted electrochemical sensor with GO@COF signal amplification for the simultaneous determination of sulfadiazine and acetaminophen. *Sensor. Actuat. B-Chem.* 300 (2019) 126993.
- [25] K.M. Sanchez. Detection and Identification of Acetaminophen (Tylenol) Metabolites using Liquid Chromatography High Resolution Mass Spectrometry (LC-HRMS/MS) Analysis. *Oregon state*. (2020) 1-20.
- [26] K.L. Muldrew, L.P. James, L. Coop, S.S. McCullough, H.P. Hendrickson and J.A. Hinson. Determination of acetaminophen-protein adducts in mouse liver and serum and human serum after hepatotoxic doses of acetaminophen using high-performance liquid chromatography with electrochemical detection. *Drug. Metab. Dispos.* 4;30 (2020) 446-51.
- [27] J. Mrochek, S. Katz, W.H. Christie and S. Dinsmore. Acetaminophen metabolism in man, as determined by high-resolution liquid chromatography. *Clin. Chem.* 8;20 (1974) 1086-96.
- [28] N.K. Al-Nemrawi and R.H. Dave. Formulation and characterization of acetaminophen nanoparticles in orally disintegrating films. *Drug. Deliv.* 2;23 (2016) 540-9.
- [29] E. Kianfar and A. Mahler. Zeolites: properties, applications, modification and selectivity. *Chapter*. (2020) 1-19.
- [30] Z. Xie and B.L. Su. Crystalline porous materials: from zeolites to metal-organic frameworks (MOFs). *Springer*. (2020) 123-6.
- [31] J.V. Smith. Topochemistry of zeolites and related materials. 1. Topology and geometry. *Chem. Rev.* 1;88 (1988) 149-82.
- [32] L.B. McCusker and C. Baerlocher. Zeolite structures. Studies in surface science and catalysis Amsterdam: Elsevier. (2007) 13-37.
- [33] M. Dusselier and M.E. Davis. Small-pore zeolites: synthesis and catalysis. *Chem. Rev.* 11;118 (2018) 5265-329.
- [34] M. Moliner, A. Corma. Advances in the synthesis of titanosilicates: from the medium pore TS-1 zeolite to highly-accessible ordered materials. *Micropor.. Mesopor.. Mat.* 189 (2014) 31-40.
- [35] R. Simancas, J.L. Jorda, F. Rey, A. Corma, A. Cantin and I. Peral. A new microporous zeolitic silicoborate (ITQ-52) with interconnected small and medium pores. *J. Am. Chem. Soc.* 9;136 (2014) 3342-5.
- [36] A. Cantin, A. Corma, S. Leiva, F. Rey J. Rius and S. Valencia. Synthesis and structure of the bidimensional zeolite ITQ-32 with small and large pores. *J. Am. Chem. Soc.* 33;127 (2005) 11560-1.
- [37] L.A. Villaescusa, J. Li, Z. Gao, J. Sun and M.A. Camblor. IDM-1: A Zeolite with Intersecting Medium and Extra-Large Pores Built as an Expansion of Zeolite MFI. *Angew. Chem.* 28; 132 (2020) 11379-82.
- [38] C.T. He, L. Jiang, Z.M. Ye, R. Krishna, Z.S. Zhong and P.Q. Liao. Exceptional hydrophobicity of a large-pore metal-organic zeolite. *J. Am. Chem. Soc.* 22;137 (2015) 7217-23.
- [39] S.U. Meshram, U.R. Khandekar, S.M. Mane and A. Mohan. Novel route of producing zeolite a resin for quality-improved detergents. *J. Surfactants. Deterg.* 2;18 (2015) 259-66.
- [40] K.B. Tankersley, N.P. Dunning, C. Carr, D.L. Lentz and V.L. Scarborough. Zeolite water purification at Tikal, an ancient Maya city in Guatemala. *Sci. Rep-Uk.* 1;10 (2020) 1-7.
- [41] N. Eroglu, M. Emekci and C.G. Athanassiou. Applications of natural zeolites on agriculture and food production. *J. Sci. Food. Agr.* 11;97 (2017) 3487-99.
- [42] L. Monasterio-Guillot, P. Alvarez-Lloret, A. Ibañez-Velasco, A. Fernandez-Martinez, E. Ruiz-Agudo and C. Rodriguez-Navarro. CO<sub>2</sub> sequestration and simultaneous zeolite production by carbonation of coal fly ash: Impact on the trapping of toxic elements. *J. CO<sub>2</sub>. Util.* 40 (2020) 101-263.
- [43] H. Zhang, Y. Kim and P.K. Dutta. Controlled release of paraquat from surface-modified zeolite Y. *Micropor. Mesopor. Mat.* 3;88 (2006) 312-8.
- [44] J.F. Zhou, J.J. Ling, G. Li, S. Zhang and D. Zhu. The molecule-level photoreactor: accurate embedded iodine-substituted boron dipyrromethene dye within zeolitic imidazolate framework-8 for highly efficient oxidization of sulfides under visible light. *Mater. Chem.* 24 (2022) 100-774.
- [45] T. Yamamoto, K. Iimura, H. Satone, K. Itoh and K. Maeda. Ozonation of aqueous phenol using high-silica zeolite in an aerated mixing vessel. *As-P. J. Chem. Eng.* 2;13 (2018) 2-175.
- [46] S. Tul Muntha, A. Kausar and M. Siddiq. A review on zeolite-reinforced polymeric membranes: salient features and applications. *Polym-Plast. Technol.* 18;55 (2016) 1971-87.

- [47] I. Švancara, K. Vytrás, J. Barek and J. Zima. Carbon paste electrodes in modern electroanalysis. *Crit. Rev. Anal. Chem.* 4;31 (2001) 311-45.
- [48] J. Zima, I. Švancara, J. Barek and K. Vytrás. Recent advances in electroanalysis of organic compounds at carbon paste electrodes. *Crit. Rev. Anal. Chem.* 3;39 (2009) 204-27.
- [49] A. Walcarius. Zeolite-modified electrodes in electroanalytical chemistry. *Anal. Chem. Acta.* 1;384 (1999) 1-16.
- [50] M. Ferreira, N.E. Sahin, A.M. Fonseca, P. Parpot and I.C. Neves. Oxidation of pollutants via an electro-Fenton-like process in aqueous media using iron-zeolite modified electrodes. *New. J. Chem.* 28; 45 (2021) 12750-7.
- [51] D.R. Rolison. Zeolite-modified electrodes and electrode-modified zeolites. *Chem. Rev.* 5;90 (1990) 867-78.
- [52] X. Xu, J. Wang and Y. Long. Zeolite-based materials for gas sensors. *Ital. Phy. So.* 12; 6 (2006) 1751-64.
- [53] A. El-Shafei, A. Abd Elhafeez and H. Mostafa. Ethanol oxidation at metal-zeolite-modified electrodes in alkaline medium. Part 2: palladium-zeolite-modified graphite electrode. *J. Solid. State. Electr.* 2; 14 (2010) 185-90.
- [54] A. Walcarius and P. Mariaulle. L. Lamberts. Zeolite-modified solid carbon paste electrodes. *J. Solid. State. Electr.* 10; 7 (2003) 671-7.
- [55] T. Rohani and M.A. Taher. A new method for electrocatalytic oxidation of ascorbic acid at the Cu (II) zeolite-modified electrode. *Talanta.* 3;78 (2009) 743-7.
- [56] W. Lutz. Zeolite Y: synthesis, modification, and properties—a case revisited. *Adv. Mater. Sci. Eng.* (2014).
- [57] J.D. Rimer, M. Kumar, R. Li, A.I. Lupulescu and M.D. Oleksiak. Tailoring the physicochemical properties of zeolite catalysts. *Catal. Sci. Technol.* 11;4 (2014) 3762-71.
- [58] K. Möller and T. Bein. Mesoporosity—a new dimension for zeolites. *Chem. Soc. Rev.* 9;42 (2013) 3689-707.
- [59] S. Sharifian and A. Nezamzadeh-Ejchieh. Modification of carbon paste electrode with Fe (III)-clinoptilolite nano-particles for simultaneous voltammetric determination of acetaminophen and ascorbic acid. *Adv. Mater. Res-Switz: C.* 58 (2016) 510-20.
- [60] S. Tajik, H. Beitollahi, S.Z. Mohammadi, M. Azimzadeh, K. Zhang and Q. Van Le. Recent developments in electrochemical sensors for detecting hydrazine with different modified electrodes. *RSC. Adv.* 51;10 (2020) 30481-98.
- [61] P.W. Ondachi. Surface modified electrodes as a novel technique for characterizing adansonia digitata fruit: *University of Nairobi.* (2000) 1-238.

# COPYRIGHTS



© 2022 by the authors. Licensee PNU, Tehran, Iran. This article is an open access article distributed under the terms and conditions of the Creative Commons Attribution 4.0 International (CC BY4.0) (<http://creativecommons.org/licenses/by/4.0>)



سنتز و ارزیابی نانو ژئولیت Na/Al به عنوان یک اصلاح کننده جدید برای اندازه گیری الکتروشیمیایی استامینوفن

افروزه عربی<sup>۱</sup>، علیرضا محدثی زرنندی<sup>۱\*</sup>، محمدعلی کریمی<sup>۱</sup>، مهدی رنجبر<sup>۲</sup>

۱. گروه شیمی، دانشگاه پیام نور، صندوق پستی ۳۶۹۷-۱۹۳۹۵ تهران، ایران

۲. مرکز تحقیقات دارویی، انستتوی نوروفورموکولوژی، دانشگاه علوم پزشکی کرمان، کرمان، ایران

تاریخ دریافت: ۲۰ دی ۱۴۰۰      تاریخ پذیرش: ۸ اسفند ۱۴۰۰

## چکیدہ

در این تحقیق، نانو زولیت‌های Na/Al (ZAN) سنتز و شناسایی شدند، سپس یک الکترود کربن اصلاح‌شده (CPE) شده با ZAN برای اندازه‌گیری استامینوفن ساخته شد. مطالعات الکتروشیمیایی با ولتامتری رفت و برگشت خطی ولتامتری پالس تفاضلی انجام شد. این الکترود اصلاح‌شده در حضور استامینوفن به دلیل خواص الکتروکاتالیستی، پیک اکسیداسیون خاصی را در ولتاژ ۵۹/۰ ولت نشان می‌دهد. حد تشخیص این روش ۵/۸ میکرومولار، انحراف استاندارد نسبی برای ۷ اندازه‌گیری تکراری ۱/۱ درصد و محدوده خطی کالبراسیون برای تعیین استامینوفن ۱۰ تا ۱۱۵ میکرومولار است.

## واژه‌های کلیدی

الکتروود اصلاح شده، ژئولیت، اندازه گیری الکتروکاتالیزوری، استامینوفن.